PAPER

Check for updates

Synthesis, characterization, and alkoxide transfer reactivity of dimeric Tl₂(OR)₂ complexes†

Amanda Grass,‡[a] Lakshani Wathsala Kulathungage,‡[a] Duleeka Wannipurage,‡[a] Maryam Yousif,[a,c] Cassandra L. Ward[b] and Stanislav Groysman (ID) *[a]

Reaction of LiOC^{t}Bu$_2$Ph with TlPF$_6$ forms the dimeric Tl$_2$(OC^{t}Bu$_2$Ph)$_2$ complex, a rare example of a homoleptic thallium alkoxide complex demonstrating formally two-coordinate metal centers. Characterization of Tl$_2$(OC^{t}Bu$_2$Ph)$_2$ by ^{1}H and ^{13}C NMR spectroscopy and X-ray crystallography reveals the presence of two isomers differing by the mutual conformation of the alkoxide ligands, and by the planarity of the central Tl–O–Tl–O plane. Tl$_2$(OC^{t}Bu$_2$Ph)$_2$ serves as a convenient precursor to the formation of old and new [M(OC^{t}Bu$_2$Ph)$_n$] complexes (M = Cr, Fe, Cu, Zn), including a rare example of T-shaped Zn(OC^{t}Bu$_2$Ph)$_2$(THF) complex, which could not be previously synthesized using more conventional LiOR/HOR precursors. The reaction of [Ru(cymene)Cl$_2$]$_2$ with Tl$_2$(OC^{t}Bu$_2$Ph)$_2$ results in the formation of a ruthenium(II) alkoxide complex. For ruthenium, the initial coordination of the alkoxide triggers C–H activation at the *ortho*-H of [OC^{t}Bu$_2$Ph] which results in its bidentate coordination. In addition to Tl$_2$(OC^{t}Bu$_2$Ph)$_2$, related Tl$_2$(OC^{t}Bu$_2$(3,5-Me$_2$C$_6$H$_3$))$_2$ was also synthesized, characterized, and shown to exhibit similar reactivity with iron and ruthenium precursors. Synthetic, structural, and spectroscopic characterizations are presented.

Introduction

Alkoxides are among the most ubiquitous ligands in coordination chemistry and homogeneous catalysis,[1–6] and therefore it is important to develop general, efficient, and reliable routes towards alkoxide-supported transition metal complexes. Two most common routes to the transition metal alkoxide complexes include salt metathesis between transition metal halide sources (MX$_n$) and alkali metal alkoxides (M′OR), or protonolysis of transition metal amide/alkyl precursors with more acidic alcohols.[7,8] Both routes exhibit advantages and drawbacks. While the salt metathesis route employs commercially available transition metal halide precursors, it often yields mixed-metal "ate" complexes of [MM′(OR)$_n$X] composition as a result of incomplete removal of M′X (M′ = Li, Na, K).[1,2,9] In contrast, protonolysis route generally forms M(OR)$_n$ complexes cleanly. However, it requires the corresponding transition metal

amide/alkyl precursors (often commercially unavailable). An alternative, less explored synthetic route to the metal–alkoxide complexes involves salt metathesis between thallium alkoxides TlOR and transition metal halides MX$_n$.[10,11] As the reaction of TlOR with halide-containing complexes yields insoluble TlX salts, this route generally avoids formation of the mixed-metal species. This route also employs commercially available transition metal halide complexes; TlOR can be synthesized in one step using the combination of TlPF$_6$ (or other non-coordinating anion) with alkali metal alkoxides.

We have previously reported syntheses of mononuclear transition metal complexes supported by bulky alkoxide ligands OR (OR = [OC^{t}Bu$_2$Ph] and [OC^{t}Bu$_2$(3,5-Ph$_2$C$_6$H$_3$)]), and their application in nitrene and carbene transfer reactions.[12] For M = Cr–Co, the reaction of MCl$_2$ with two equivalents of LiOC^{t}Bu$_2$Ph produced "seesaw clusters" of the M$_2$Li$_2$Cl$_2$(OC^{t}Bu$_2$Ph)$_4$ form.[13] Subsequent treatment of these clusters with TlPF$_6$ yielded M(OC^{t}Bu$_2$Ph)$_2$(THF)$_2$ complexes for M = Mn, Fe, Co in moderate yields (overall yields between 30–40%).[14] For Cr, the second step of the procedure (treatment of Cr$_2$Li$_2$Cl$_2$(OC^{t}Bu$_2$Ph)$_4$ with TlPF$_6$) failed to produce the desired chromium(II) bis(alkoxide) product. A different synthetic route, involving previously reported Cr(N(SiMe$_3$)$_2$)$_2$(THF)$_2$[15] (also synthesized from CrCl$_2$) was undertaken, and found to yield Cr$_2$(OC^{t}Bu$_2$Ph)$_4$ dimer.[16] We hypothesized that the synthesis of [M(OC^{t}Bu$_2$Ph)$_2$] complexes can be improved by utilizing a single-step salt metathesis reaction of MCl$_2$ with

*a*Department of Chemistry, Wayne State University, 5101 Cass Ave., Detroit, MI 48202, USA. E-mail: groysman@wayne.edu
*b*Lumigen Instrument Center, Wayne State University, 5101 Cass Avenue, Detroit, Michigan 48202, USA
*c*Department of Chemistry, Grand Valley State University, 1 Campus Drive, 312 Padnos Hall, Allendale, Michigan 49401, USA
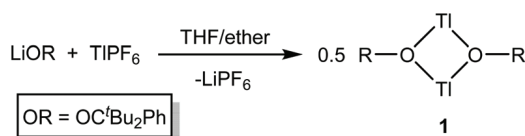
TlOC^{t}Bu$_2$Ph. Furthermore, our previous synthetic endeavors failed to produce [Ni(OC^{t}Bu$_2$Ph)$_2$] and [Zn(OC^{t}Bu$_2$Ph)$_2$] species, yielding unreactive [M(OC^{t}Bu$_2$Ph)$_2$(Cl)Li] complexes.[14,17] It was hypothesized that the substitution of LiOC^{t}Bu$_2$Ph by TlOC^{t}Bu$_2$Ph would avoid the formation of stable heterobimetallic intermediates [MM′(OC^{t}Bu$_2$Ph)$_n$X] and would drive the reaction towards [M(OC^{t}Bu$_2$Ph)$_2$] species (and TlX). In this manuscript, we describe synthetic, spectroscopic and structural investigation of a new thallium complex with bulky alkoxide ligand [OC^{t}Bu$_2$Ph], which adopts a dimeric alkoxide-bridged structure Tl$_2$(OC^{t}Bu$_2$Ph)$_2$. We also demonstrate that Tl$_2$(OC^{t}Bu$_2$Ph)$_2$ can be used as a precursor in the synthesis of Cr, Fe, and Cu alkoxide complexes in one step, and leads to the previously inaccessible complexes with Zn and Ru.

Results and discussion

Synthesis and characterization of Tl$_2$(OC^{t}Bu$_2$Ph)$_2$

Mixing THF solutions of TlPF$_6$ and LiOC^{t}Bu$_2$Ph[13] at room temperature produced silver-gray suspension that was stirred for 3 hours (Scheme 1). Subsequent solvent removal followed by recrystallization from hexane resulted in crystalline **1** in 56% yield (average of five experiments). **1** is stable in the solid state in the absence of light at −35 °C over at least one month. It slowly decomposes in solution as indicated by the formation of a silver precipitate. ^{1}H NMR spectrum of **1** (C$_6$D$_6$, room temperature) contained one dominant species (~90%) characterized by five broad aromatic and one aliphatic (^{t}Bu) signals, indicating a single type of [OC^{t}Bu$_2$Ph] ligand with restricted phenyl rotation.[18] One of the aromatic signals overlapped with the solvent (benzene) peak, and was confirmed by homonuclear correlation spectroscopy (COSY). Close examination of ^{1}H NMR spectrum revealed the presence of additional, minor species (<10%) (^{t}Bu signal at 1.16 ppm, Fig. S1 in ESI†). Collecting ^{1}H NMR spectrum in toluene-d$_8$ demonstrated different (approximately 60 : 40) ratio between the two species, as indicated by two ^{t}Bu peaks at 1.23 and 1.16 ppm (Fig. S3, ESI†). A similar pattern was observed for the aromatic signals, most of which appear broad. Variable temperature (VT) NMR studies (toluene-d$_8$) demonstrated the presence of two isomers down to −40 °C (Fig. 1); coalescence into single species was observed above room temperature. The isomers were assigned assuming that **1b** is a major isomer in both C$_6$D$_6$ and C$_7$D$_8$, and based on the fact that **1b** was isolated in a pure state and structurally characterized (see below).

The X-ray crystallographic study rationalized spectroscopic observations revealing the presence of two structural isomers.
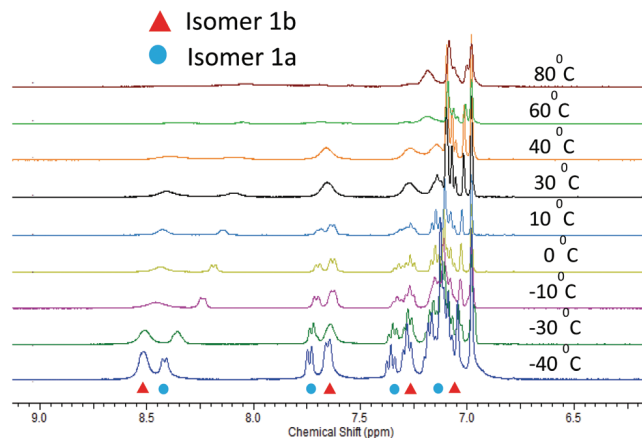

Fig. 1 VT NMR (toluene-d$_8$, aromatic region) demonstrating the presence of two isomers of Tl$_2$(OC^{t}Bu$_2$Ph)$_2$.

The isomers were observed as two polymorphic structures (**1a** and **1b**) both adopting a dimeric Tl$_2$(μ-OC^{t}Bu$_2$Ph)$_2$ form (Fig. 2). **1a** was obtained by recrystallization of Tl$_2$(OC^{t}Bu$_2$Ph)$_2$ as prepared; crystals of **1b** were obtained in an attempt to make the [Ni(OC^{t}Bu$_2$Ph)$_2$] complex (see below). In both complexes, Tl(I) centers are formally two-coordinate. However, both complexes exhibit additional agostic interactions as indicated by the Tl⋯H–C distances in the range of 2.7–3.0 Å (see Fig. S42 in ESI†).[19] We note that formally two-coordinate dimeric homoleptic Tl alkoxides are exceedingly rare. Selected structures of homoleptic [TlOR]$_n$ complexes are given in Fig. 3. For non-bulky alkoxides, TlOR usually adopt tetrameric cubane structures [Tl(OR)]$_4$ (in which Tl is three-coordinate),[20,21] or lead to higher-nuclearity clusters [Tl(OR)]$_n$ (Tl featuring coordination number of 4 or higher).[22] Bulkier [OC(CH$_3$)$_3$] and [O(C(CF$_3$)$_3$)] ligands have been also shown to form tetrameric
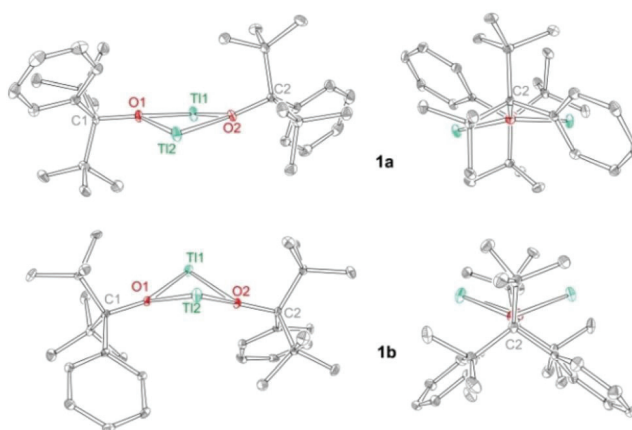

Fig. 2 X-ray structures of two structural isomers of **1**, **1a** (top, side view and front view) and **1b** (bottom, side view and front view), 50% probability ellipsoids. H atoms are omitted for clarity. Selected bond distances (Å) for **1a**: Tl1−O1 2.389(2), Tl1−O2 2.402(2), Tl2−O2 2.396(2), Tl2−O1 2.399(2), Tl1⋯Tl3.6647(4), O1⋯O2 3.045(2). Selected bond distances (Å) for **1b**: Tl1−O1 2.363(3), Tl1−O2 2.432(3), Tl2−O2 2.372(3), Tl2−O1 2.423(3), Tl1⋯Tl2 3.5646(3), O1⋯O2 2.922(3).
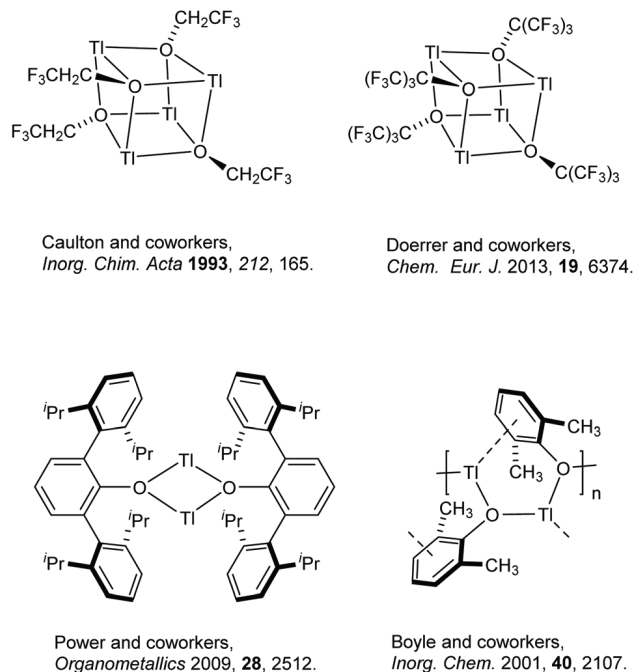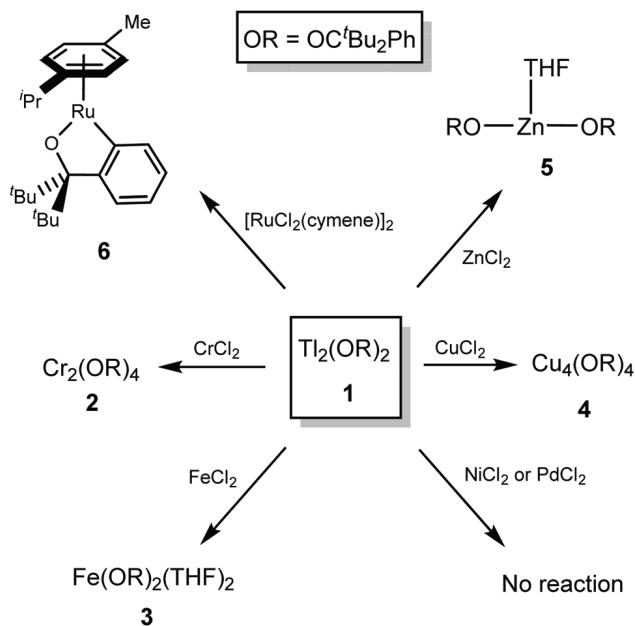
Scheme 1 Synthesis of Tl$_2$(OC^{t}Bu$_2$Ph)$_2$ (**1**).

Fig. 3 Selected examples of homoleptic TlOR/TlOAr structures.

Scheme 2 Alkoxide-transfer reactions of Tl$_2$(OC^{t}Bu$_2$Ph)$_2$ to obtain compounds **2–6**.

cubane structures [Tl(OR)]$_4$ featuring a three-coordinate Tl.[23,24] In contrast, bulky 2,6-disubstituted aryloxides were shown to form dimeric formally two-coordinate Tl$_2$(OAr)$_2$ readily.[25–28] Less bulky aryloxides typically formed higher-nuclearity clusters or polymers,[29–32] except for the noteworthy example of electron-deficient aryloxides, such as in Tl$_2$(O(p-C$_6$H$_4$F))$_2$.[27]

While both **1a** and **1b** contain dimeric Tl$_2$(μ_2-OC^{t}Bu$_2$Ph)$_2$ structural units, there are notable differences between the structures. Most previously reported dimeric Tl$_2$(OAr)$_2$ structures exhibited planar, or nearly planar, Tl$_2$O$_2$ rings. Whereas **1a** displays only relatively small deviation from planarity (angle of 19° between Tl1–O1–Tl2 and Tl2–O2–Tl1 planes), the deviation from planarity in **1b** becomes more substantial (angle of 49° between Tl1–O1–Tl2 and Tl2–O2–Tl1 planes). What is the origin of the differences between torsion angles in **1a** and **1b**? Unlike aryloxides, which tend to have preferred conformation due to their planar nature, alkoxides (featuring three comparable substituents) are expected to be conformationally labile, especially when coordinated to a main-group element. Looking down the C1–C2 vector in **1a** reveals sterically favorable staggered conformation in **1a** (Fig. 2, top right). In contrast, **1b** exhibits eclipsed conformation between the alkoxides substituents. Of the three substituents interacting between two different alkoxides (Fig. 2, bottom right), two bottom substituents exhibit less energetic anticlinal eclipsed relationship positioning ^{t}Bu on one half of **1b** in front of the phenyl on the other half. In contrast, two top ^{t}Bu are synperiplanar, which is the most sterically demanding interaction. To increase the distance between these two substituents, the angle between the Tl1–O1–Tl2 and Tl2–O2–Tl1 increases.

Alkoxide-transfer reactivity of Tl$_2$(OC^{t}Bu$_2$Ph)$_2$

Following the synthesis and the characterization of Tl$_2$(OC^{t}Bu$_2$Ph)$_2$, its potential as an alkoxide-transfer reagent with various transition metal chlorides was evaluated (Scheme 2). Treatment of CrCl$_2$ and FeCl$_2$ with **1** produced previously reported complexes Cr$_2$(OC^{t}Bu$_2$Ph)$_4$ (**2**, 64% yield)[16] and Fe(OC^{t}Bu$_2$Ph)$_2$(THF)$_2$ (**3**, 51% yield).[33] Their compositions were confirmed by unit cell measurements and UV-vis spectra. The reaction of CuCl$_2$ with Tl$_2$(OC^{t}Bu$_2$Ph)$_2$ produced the Cu(I) product Cu$_4$(OC^{t}Bu$_2$Ph)$_4$ (**4**, 39% yield), as previously observed for the reaction of CuCl$_2$ with LiOC^{t}Bu$_2$Ph.[14]

We have also investigated the potential of Tl$_2$(OC^{t}Bu$_2$Ph)$_2$ to form new bis(alkoxide) complexes, which could not be obtained previously via the LiOC^{t}Bu$_2$Ph/HOC^{t}Bu$_2$Ph routes. Treatment of NiCl$_2$ with Tl$_2$(OC^{t}Bu$_2$Ph)$_2$ resulted in the re-isolation of Tl$_2$(OC^{t}Bu$_2$Ph)$_2$. These results are consistent with the previously observed lack of reactivity between [Ni(OC^{t}Bu$_2$Ph)(μ-OC^{t}Bu$_2$Ph)(μ-Cl)Li(THF)$_2$] and TlPF$_6$.[14] Notably, a single isomer was observed in this case by ^{1}H NMR (Fig. S17†); crystal structure determination revealed the structure of **1b** (Fig. 2). For Zn, we have previously reported that the reaction of ZnEt$_2$ with HOC^{t}Bu$_2$Ph failed to produce the desired bis(alkoxide) complex, whereas treatment of ZnCl$_2$ with two equivalents of LiOC^{t}Bu$_2$Ph formed colorless Zn(Cl)(μ_2-OC^{t}Bu$_2$Ph)$_2$Li(THF).[17] Treatment of ZnCl$_2$ with Tl$_2$(OC^{t}Bu$_2$Ph)$_2$ yielded the new product **5**, which was obtained as colorless crystals from hexane (64% yield). The ^{1}H NMR characterization of **5** suggested formation of a zinc bis(alkoxide) tetrahydrofuran complex containing approximately a 2:1 ratio between [OC^{t}Bu$_2$Ph] and THF ligands.

X-ray structure determination confirmed Zn(OC^{t}Bu$_2$Ph)$_2$(THF) composition for **5**. The structure (Fig. 4) revealed T-shaped
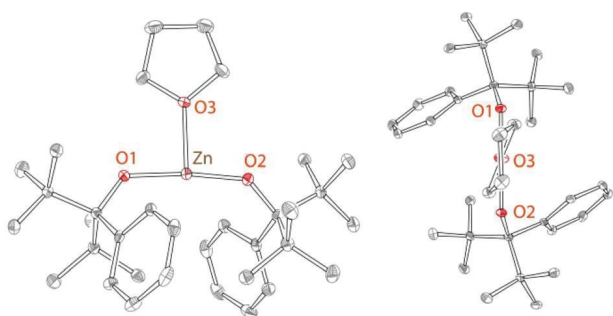
Fig. 4 X-ray structure of **5**, 50% probability ellipsoids. H atoms are omitted for clarity. Selected bond distances (Å): Zn−O1 1.819(2), Zn−O2 1.825(2), Zn−O3 2.094(2). Selected bond angles (°): O1−Zn−O2 173.12 (7), O1−Zn−O3 96.19(7), O2−Zn−O3 90.69(7).

complex of approximate (non-crystallographic) C_2 symmetry. The alkoxide oxygens demonstrate nearly linear disposition (O1−Zn−O2 173.1(1)°), while the angles between alkoxides and the remaining THF ligands are close to 90° (see Fig. 4 for structural details). Complex **5** is a rare example of a T-shaped Zn complex featuring alkoxide ligation. Cambridge Structural Database contains over 1000 examples of three-coordinate Zn complexes, of which only very few mononuclear examples demonstrated nearly T-shaped geometry (interligand angle of ~160°) (Fig. 5).[34–36] Several additional three-coordinate zinc complexes exhibited distorted trigonal geometries approaching T-shaped (angles ~150° or slightly below).[37–40] In contrast, alkoxide- (or aryloxide) ligated three-coordinate zinc complexes generally feature trigonal planar geometry.[17,41–45] To the best of our knowledge, complex **3** exhibits the most linear interligand RO−Zn−OR angle for any T-shaped mononuclear Zn complex.

We have also explored the reactivity of Tl$_2$(OC^{t}Bu$_2$Ph)$_2$ towards heavier (4d) middle/late metals in the alkoxide ligand environment. This work specifically focused on M(II) complexes (M = Ru, Pd); complexes of both metals with unsupported alkoxide ligands are relatively rare.[1,46–50] Treatment of [RuCl$_2$(cymene)]$_2$ with Tl$_2$(OC^{t}Bu$_2$Ph)$_2$ resulted in the formation of a magenta solution, from which dark-purple crystals were isolated. ^{1}H NMR characterization of the crystalline product **6** (76% yield) demonstrated the presence of only four aromatic alkoxide signals, instead of the expected five phenyl protons of [Tl$_2$(OC^{t}Bu$_2$Ph)$_2$]. In addition, the NMR spectrum contained cymene aromatic protons as two doublets at 5.17 and 5.05 ppm, one ^{t}Bu resonance (18 protons overall) at 1.18 ppm, cymene ^{i}Pr resonances at 1.02 and 2.09 ppm, and the cymene Me peak at 1.57 ppm. X-ray diffraction study disclosed the structure of C−H activated product **6** (Fig. 6, left). **6** features bidentate coordination of the alkoxide through oxygen and the *ortho*-carbon to Ru(II) center, in addition to the η[6]-bound cymene ligand. No reaction was observed between PdCl$_2$ and Tl$_2$(OC^{t}Bu$_2$Ph)$_2$.

Synthesis and reactions of Tl$_2$(OC^{t}Bu$_2$(3,5-Me$_2$C$_6$H$_3$))$_2$

Thallium-mediated alkoxide-transfer protocol was explored with one additional bulky alkoxide ligand, [OC^{t}Bu$_2$(3,5-

Power & Shoner,
Angew. Chem. Int. Ed. Engl. 1990, **29**, 1403.

Bochman and coworkers,
Inorg. Chem. 1994, **33**, 2290.

Power and coworkers,
Inorg. Chem. 1995, **34**, 49.

Hevia and coworkers,
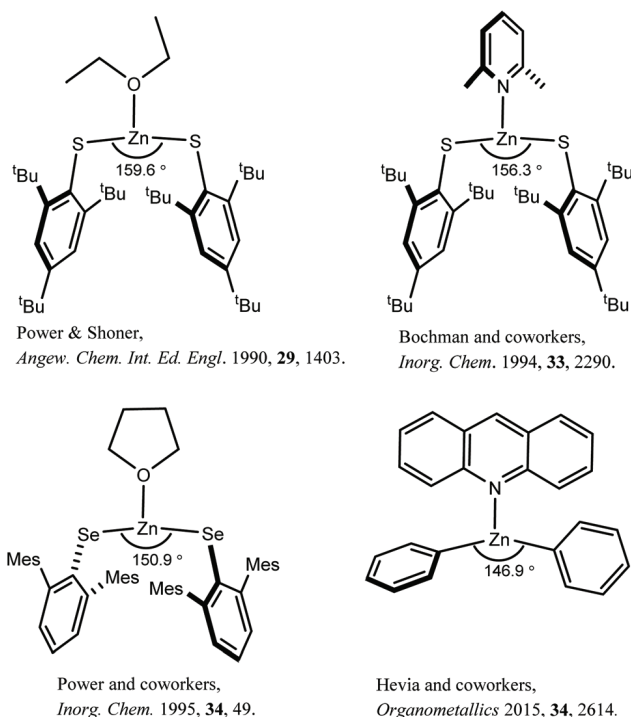*Organometallics* 2015, **34**, 2614.

Fig. 5 Previously reported three-coordinate Zn complexes featuring geometry close to T-shape.
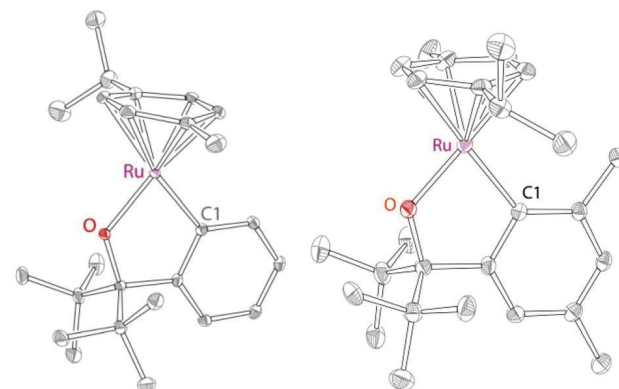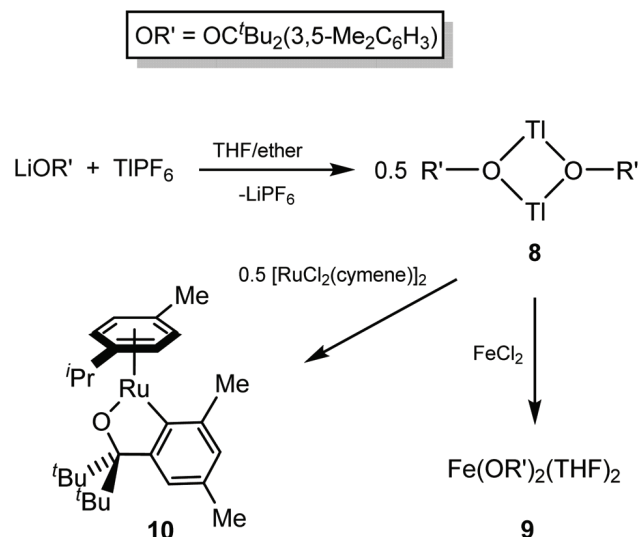

Fig. 6 X-ray structures of **6** (left) and **10** (right), 50% probability ellipsoids. H atoms are omitted for clarity. Selected bond distances (Å) and angles (°) for **6**: Ru−O 1.933(2), Ru−C1 2.027(2), O−Ru−C1 80.94(7). Selected bond distances (Å) and angles (°) for **10**: Ru−O 1.910(1), Ru−C1 2.068(2), O−Ru−C1 81.32(5).

Me$_2$C$_6$H$_3$)]. Tl$_2$(OC^{t}Bu$_2$(3,5-Me$_2$C$_6$H$_3$))$_2$ (**8**) was prepared by the reaction between Li$_2$(OC^{t}Bu$_2$(3,5-Me$_2$C$_6$H$_3$))$_2$(THF)$_2$ (**7**, Fig. S43†) and TlPF$_6$ (Scheme 3) and obtained in 69% yield as colorless crystals. Similarly to Tl$_2$(OC^{t}Bu$_2$Ph)$_2$, characterization of freshly crystallized Tl$_2$(OC^{t}Bu$_2$(3,5-Me$_2$C$_6$H$_3$))$_2$ by ^{1}H NMR spectroscopy revealed the presence of two isomers (Fig. S27†). Notably, prolonged storage (4 weeks) of **8** in solution at −35 °C led to the formation of a single isomer (Fig. S24†), whose structure is shown in Fig. 7. The structure of **8** is similar to **1b**, featuring non-planar Tl$_2$O$_2$ ring and (nearly) eclipsed confor-

OR' = OC^{t}Bu$_2$(3,5-Me$_2$C$_6$H$_3$)

Scheme 3   Synthesis and reactivity of Tl$_2$(OC^{t}Bu$_2$(3,5-Me$_2$C$_6$H$_3$))$_2$ (8).
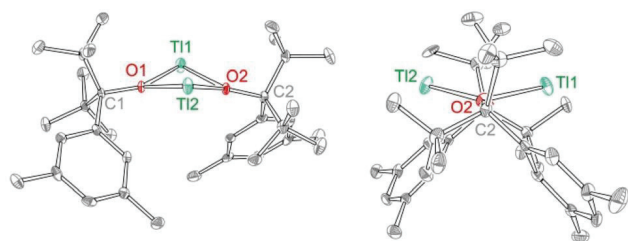

Fig. 7   X-ray structures of 8 (side view and front view), 50% probability ellipsoids. H atoms are omitted for clarity. Selected bond distances (Å): Tl1–O1 2.361(4), Tl1–O2 2.394(4), Tl2–O2 2.366(4), Tl2–O1 2.406(4), Tl1⋯Tl 3.6256(4), O1⋯O2 2.959(4).

mation between the alkoxides. Similarly to **1**, **8** serves as a convenient precursor for the synthesis of transition metal alkoxide complexes. We specifically pursued two different reaction outcomes enabled by **1**, namely the formation of an iron bis(alkoxide) complex, and bidentate alkoxoaryl ruthenium complex. Treatment of **8** with FeCl$_2$ produced Fe(OC^{t}Bu$_2$(3,5-Me$_2$C$_6$H$_3$))$_2$ (THF)$_2$ (**9**, 61%) and the reaction of **8** with [RuCl$_2$(cymene)]$_2$ produced complex **10** (81%). The structures of **9** and **10** (Fig. 8 and 6) are closely related to the structures of **3** and **6**; selected structural parameters are given in Fig. 6 and 8.

In summary, we have reported the synthesis of rare dimeric thallium–alkoxide complexes bearing bulky alkoxides [OC^{t}Bu$_2$Ph] and [OC^{t}Bu$_2$(3,5-Me$_2$C$_6$H$_3$)], Tl$_2$(OC^{t}Bu$_2$Ph)$_2$ and Tl$_2$(OC^{t}Bu$_2$(3,5-Me$_2$C$_6$H$_3$))$_2$. The complexes are observed as two different conformers; the distinct conformers are supported by VT ^{1}H NMR spectroscopy. Tl$_2$(OR)$_2$ precursors allow a one-step formation of transition metal complexes with bulky alkoxide ligands, [OC^{t}Bu$_2$Ph] and [OC^{t}Bu$_2$(3,5-Me$_2$C$_6$H$_3$)], which is generally more efficient and higher-yielding compared with the previously described two-step synthesis. Furthermore, the use of Tl$_2$(OC^{t}Bu$_2$Ph)$_2$ enabled preparation of the mononuclear T-shaped Zn(OC^{t}Bu$_2$Ph)$_2$(THF) species, as well as rare
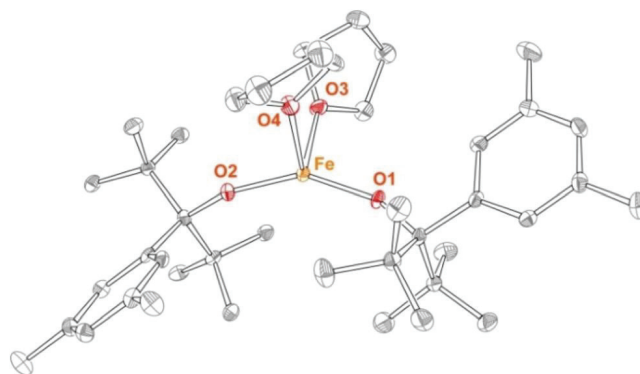

Fig. 8   X-ray structure of 9, 50% probability ellipsoids. H atoms are omitted for clarity. Selected bond distances (Å): Fe–O1 1.846(2), Fe–O2 1.851(2), Fe–O3 2.171(2), Fe–O4 2.232(2). Selected bond angles (°): O1–Fe–O2 148.1(1), O3–Fe–O4 88.8(1).

examples of the second-row complex (Ru) with both [OC^{t}Bu$_2$Ph] and [OC^{t}Bu$_2$(3,5-Me$_2$C$_6$H$_3$)]. In our future studies, we will continue exploring the reactivity of these and other Tl alkoxides (such as [OC^{t}Bu$_2$(3,5-Ph$_2$C$_6$H$_3$)][51]) with the second- and third-row middle and late transition metals.

Experimental

General methods and procedures

All reactions involving air-sensitive materials were executed in a nitrogen-filled glovebox or by standard Schlenk line procedures. Nickel(II) chloride dimethoxyethane was purchased from Sigma-Aldrich. Thallium hexafluorophosphate and anhydrous chromium chloride were purchased from Strem. The synthesis of LiOC^{t}Bu$_2$Ph was reported previously.[13] All solvents were purchased from Fischer Scientific and were of HPLC grade. The solvents were purified using an MBRAUN solvent purification system and stored over 3 Å molecular sieves. Deuterated benzene (C$_6$D$_6$) and toluene (C$_7$D$_8$) were purchased from Cambridge Laboratories, degassed under argon, and stored over 3 Å molecular sieves. NMR spectra were recorded at the Lumigen Instrument Center (Wayne State University). NMR was performed on Agilent 400 MHz or Agilent 600 MHz Spectrometers in C$_6$D$_6$ and C$_7$D$_8$ at room temperature unless otherwise noted. Chemical shifts and coupling constants (J) were reported in parts per million (δ) and hertz (Hz), respectively. IR spectra were recorded on Shimadzu IR-Affinityl FT-IR spectrometer as paratone oil mull suspensions. UV-Vis spectra were obtained using Shimadzu UV-1800 spectrometer.

Warning: Thallium hexafluorophosphate and other thallium salts are highly toxic, can be fatal if swallowed or inhaled and should be handled with utmost care! All reactions that involved thallium precursors or products were conducted in the glovebox. All thallium-contaminated waste (including glassware such as vials and pipets or kimwipes) was separated from the other glovebox waste and discarded separately labelled "thallium waste".

X-ray crystallographic details

The structures of complexes **2**,[16] **3**,[33] and **4**[14] were reported previously. The structures of **1a**, **1b**, **5–10** were determined by X-ray diffraction analysis. The crystals were mounted on a Bruker APEXII/Kappa goniometer platform diffractometer equipped with an APEX II detector. A graphic monochromator was employed for wavelength selection of the Mo Kα radiation (λ = 0.71073 Å). The data were processed and the structures were solved using the APEX 3 software supplied by Bruker AXS. The structures were refined with the program ShelXL using Olex2.[52,53] Hydrogen atoms were placed in calculated positions using a standard riding model and refined isotropically; all other atoms were refined anisotropically. The structure of **1b** exhibited high residual electron density in the vicinity of heavy metal (Tl) centers, likely due to the imperfect absorption correction. The structure of **10** exhibited *tert*-butyl groups disorder which was successfully modeled by two alternating conformations. Selected crystal and structure refinement data is given in Table S1 (ESI†).

Synthesis of Tl$_2$(OC^{t}Bu$_2$Ph)$_2$ (1)

A solution of TlPF$_6$ (100 mg, 0.287 mmol) in THF was added to a stirred clear ether solution of LiOC^{t}Bu$_2$Ph (63 mg, 0.276 mmol) at room temperature. The reaction turned silver-grey and was stirred at room temperature for three hours. The volatiles were removed *in vacuo*. The resulting solid was dissolved in hexane, filtered, and concentrated. Subsequent recrystallization at −35 °C yields X-ray quality crystals of **1** as two polymorphs **1a** and **1b** in 56% yield (average over five experiments, range between 49% and 62%). Scaled-up synthesis: A solution of LiOC^{t}Bu$_2$Ph (250 mg, 1.115 mmol) in ether was added to a stirred clear THF solution of TlPF$_6$ (400 mg, 1.152 mmol) at room temperature. The reaction turned silver-grey and was stirred at room temperature for three hours. The volatiles were removed *in vacuo*. The resulting solid was dissolved in hexane, filtered, and concentrated. Subsequent recrystallization at −35 °C yields X-ray quality crystals of **1** (218 mg, 46% yield). ^{1}H NMR (600 MHz, C$_6$D$_6$, room temperature) δ 8.52 (bs, 1H, Ph), 7.68 (bs, 1H, Ph), 7.29 (bs, 1H, Ph), 7.15 (bs, 1H, Ph), 7.10 (bs, 1H, Ph), 1.26 (s, 18H) ppm. ^{1}H NMR (400 MHz, C$_7$D$_8$, room temperature) δ 8.42 (bs, 1H, Ph), 8.10 (bs, 1H, Ph), 7.67 (bs, 2H, Ph), 7.27 (bs, 2H, Ph), 7.14 (t, $^3J_{HH}$ = 7 Hz, 2H, Ph), 7.09 (m, 2H, Ph), 1.23 (s, 18H), 1.16 (s, 10H) ppm. ^{1}H NMR (400 MHz, C$_7$D$_8$, −40 °C) δ 8.53 (bs, 1H, Ph), 8.44 (d, $^3J_{HH}$ = 6.7 Hz, 1H, Ph), 7.76 (d, $^3J_{HH}$ = 7.8 Hz, 1H, Ph), 7.68 (d, $^3J_{HH}$ = 7.4 Hz, 1H, Ph), 7.37 (t, $^3J_{HH}$ = 7.6 Hz, 1H, Ph), 7.30 (t, $^3J_{HH}$ = 7.2 Hz, 1H, Ph), 7.18 (m, 2H, Ph), 7.11 (m, 2H, Ph), 1.27 (s, 18H), 1.17 (s, 6H) ppm. ^{13}C NMR (C$_6$D$_6$, 150 MHz) δ 152.78, 130.59, 129.55, 126.53, 125.60, 125.36, 89.80, 43.62, 31.53 ppm. UV-vis: λ_{max}, nm (ε_M, L mol^{-1} cm^{-1}) 311 (3100), 294 (3300), 261 (sh, 6500).

Synthesis of Cr$_2$(OC^{t}Bu$_2$Ph)$_4$ (2)

A solution of Tl$_2$(OC^{t}Bu$_2$Ph)$_2$ (70 mg, 0.083 mmol) in THF was added to a stirring THF solution of CrCl$_2$ (8 mg, 0.066 mmol)

at room temperature. The reaction turned cloudy grey with a tinge of light green. The reaction was stirred at room temperature for 90 minutes. The volatiles were removed *in vacuo*. The resulting residue was dissolved in hexane, filtered, and concentrated. Subsequent recrystallization at −35 °C yields light green X-ray quality crystals of the previously characterized Cr$_2$(OC^{t}Bu$_2$Ph)$_4$[16] (21 mg, 64% yield).

Synthesis of Fe(OC^{t}Bu$_2$Ph)$_2$(THF)$_2$ (3)

A solution of Tl$_2$(OC^{t}Bu$_2$Ph)$_2$ (190 mg, 0.222 mmol) in THF was added to a stirring THF solution of FeCl$_2$ (28 mg, 0.222 mmol) at room temperature. The solution color turned into brownish white. The reaction was stirred at room temperature for one hour. The volatiles were removed *in vacuo*. The resulting residue was dissolved in hexane, filtered, and concentrated. Recrystallization from hexane at −35 °C yielded white X-ray quality crystals of the previously synthesized Fe(OC^{t}Bu$_2$Ph)$_2$(THF)$_2$[33] (72 mg, 51% yield). The nature of the product was confirmed by the unit cell measurements.

Synthesis of Cu$_4$(OC^{t}Bu$_2$Ph)$_4$ (4)

A solution of Tl$_2$(OC^{t}Bu$_2$Ph)$_2$ (85 mg, 0.100 mmol) in THF was added to a stirring THF solution of CuCl$_2$ (13 mg, 0.10 mmol) at room temperature. The solution turned into deep red immediately and then into brown. The reaction was stirred at room temperature for one hour. The volatiles were removed *in vacuo*. The resulting residue was dissolved in hexane, filtered, and concentrated. Recrystallization from hexane at −35 °C yielded colorless crystals of the previously synthesized Cu$_4$(OC^{t}Bu$_2$Ph)$_4$[14] (11 mg, 39% yield). The nature of the product was confirmed by ^{1}H NMR spectrum (see ESI†).

Synthesis of Zn(OC^{t}Bu$_2$Ph)$_2$(THF) (5)

A solution of Tl$_2$(OC^{t}Bu$_2$Ph)$_2$ (170 mg, 0.200 mmol) in THF was added to a stirred THF solution of ZnCl$_2$ (27 mg, 0.200 mmol) at room temperature. The initially transparent solution turned into milky white suspension. The reaction was stirred at room temperature for one hour. The volatiles were removed *in vacuo*. The residue was dissolved in hexane, filtered, and concentrated. Recrystallization from hexane at −35 °C yielded colorless crystals of **5** (74 mg, 64% yield). ^{1}H NMR (C$_6$D$_6$, 400 MHz) δ 7.92 (d, J_{HH} = 7.8 Hz, 2H, Ph), 7.65 (m, 2H, Ph), 7.18 (m, 2H, Ph), 7.09 (m, 4H, Ph), 3.73 (m, 4H, THF), 1.33 (m, 4H, THF), 1.23 (s, 36H) ppm. ^{13}C NMR (C$_6$D$_6$, 100 MHz) δ 151.25, 130.14, 127.89, 126.04, 125.94, 85.17, 69.66, 43.09, 31.58, 25.84 ppm. IR (cm^{-1}): 2970 (w), 2940 (w), 2878 (w), 2832 (w), 1489 (w), 1389 (w), 1366 (w), 1088 (w), 1057 (m), 988 (m), 748 (s), 710 (s).

Synthesis of Ru(cymene)(κ^2-OC^{t}Bu$_2$C$_6$H$_2$) (6)

A solution of Tl$_2$(OC^{t}Bu$_2$Ph)$_2$ (85 mg, 0.100 mmol) in THF was added to a stirred THF solution of [Ru(p-cymene)Cl$_2$]$_2$ (31 mg, 0.050 mmol) at room temperature. Following the addition, the color of the solution turned magenta and precipitate formation was observed. The reaction was stirred at room temperature for one hour. The volatiles were removed *in vacuo*. The

resulting residue was dissolved in hexane, filtered, and concentrated. Recrystallization from hexane at −35 °C yielded dark purple crystals of **6** (34 mg, 76% yield). ^{1}H NMR (C_6D_6, 600 MHz) δ 8.88 (d, J_{HH} = 7.6 Hz, 1H, Ph), 7.52 (d, J_{HH} = 7.9 Hz, 1H, Ph), 7.20 (t, J_{HH} = 7.2 Hz, 1H, Ph), 7.00 (m, 1H, Ph), 5.17 (d, J_{HH} = 5.6 Hz, 2H, cymene), 5.05 (d, J_{HH} = 5.6 Hz, 2H, cymene), 2.09 (m, 1H, cymene), 1.57 (s, 3H, cymene), 1.18 (s, 18H, ^{t}Bu), 1.02(d, J_{HH} = 5.9 Hz, 6H) ppm. ^{13}C NMR (C_6D_6, 150 MHz) δ 178.44, 168.41, 139.79, 124.45, 124.08, 122.31, 106.74, 96.84, 84.48, 81.77, 80.43, 39.33, 32.24, 31.03, 23.09, 19.99 ppm. UV-vis: λ_{max}, nm (ε_M, L mol^{-1} cm^{-1}): 539 (2800), 355 (8600), 296 (sh, 13 400), 256 (28 300). Anal. calcd for $C_{25}H_{36}ORu \cdot 0.5H_2O$: C, 64.90; H, 8.06. Found: C, 64.86; H, 7.77.

Synthesis of LiOC^{t}Bu$_2$(3,5-Me$_2$C$_6$H$_3$) (7)

To a solution of 1-bromo-3,5-dimethylbenzene (0.430 g, 2.33 mmol) in 4 ml ether and 2 ml THF, a solution of *t*-BuLi in pentane (2.7 ml, 1.7 M) was added dropwise at −35 °C. The solution changed color from colorless to yellow. The reaction was allowed to slowly warm to room temperature while stirred for one hour, after which it was cooled again to −35 °C and added to a cold solution of hexamethylacetone (0.4 mL, 2.31 mmol) in 2 ml of ether. The reaction was stirred for 24 hours, after which all solvents were removed under *in vacuo* to yield yellowish white residue. The residue was dissolved in hexanes and kept at −35 °C to get colorless crystals of **7** (428 mg, 81% yield). ^{1}H NMR (600 MHz, C_6D_6, room temperature) δ 7.67 (s, 1H, Ph), 7.43 (s, 1H, Ph), 6.75 (s, 1H, Ph), 2.30 (s, 3H, Me), 2.19 (s, 3H, Me), 1.19 (s, 18H, ^{t}Bu) ppm. ^{13}C NMR (C_6D_6, 150 MHz) δ 152.80, 137.63, 136.02, 125.46, 85.46, 43.04, 32.05, 22.42 ppm. IR (cm^{-1}): 2962 (m), 2870 (m), 2816 (w), 1604(w), 1481 (w), 1388 (w), 1365 (w), 1126 (w), 1080 (s), 1010 (m), 849 (s), 764 (s), 709 (s). The structure of **7** was also confirmed by the X-ray structure determination (see ESI†).

Synthesis of Tl$_2$(OCBu$_2$(3,5-Me$_2$C$_6$H$_3$))$_2$ (8)

A solution of TlPF$_6$ (89 mg, 0.255 mmol) in THF was added to a stirred clear THF solution of LiOC^{t}Bu$_2$(3,5-Me$_2$Ph) (65 mg, 0.256 mmol) at room temperature. The reaction turned silver-grey and was stirred at room temperature for two hours. The volatiles were removed *in vacuo*. The resulting solid was dissolved in hexane, filtered, and concentrated. Subsequent recrystallization at −35 °C yields colorless crystals of **8** (79 mg, 69% yield). ^{1}H NMR (600 MHz, C_6D_6, room temperature) δ 8.14 (bs, 1H, Ph), δ 7.42 (bs, 1H, Ph), δ 6.74 (bs, 1H, Ph), δ 2.25 (s, 6H, Me) δ 1.26 (s, 18H, ^{t}Bu) ppm. ^{13}C NMR (C_6D_6, 150 MHz) δ 153.35, 136.17, 135.52, 129.69, 128.84, 127.89, 90.42, 44.65, 32.65, 22.66 ppm. UV-vis: λ_{max}, nm (ε_M, L mol^{-1} cm^{-1}) 316 (900), 297 (1200). The structure of **8** was also confirmed by the X-ray structure determination.

Synthesis of Fe(OC^{t}Bu$_2$(3,5-Me$_2$C$_6$H$_3$))$_2$(THF)$_2$ (9)

A solution of Tl$_2$(OC^{t}Bu$_2$(3,5-Me$_2$C$_6$H$_3$))$_2$ (190 mg, 0.210 mmol) in THF was added to a stirred THF solution of FeCl$_2$ (27 mg, 0.210 mmol) at room temperature. The solution color turned into light brown, and white precipitate formation was observed. The reaction was stirred at room temperature for one hour. The volatiles were removed *in vacuo*. The resulting residue was dissolved in hexane, filtered, and concentrated. Recrystallization from hexane at −35 °C yielded light yellow X-ray quality crystals of **9** (82 mg, 61% yield). UV-vis: λ_{max}, nm (ε_M, L mol^{-1} cm^{-1}) 407 (sh, 250). IR (cm^{-1}): 2970 (w), 2978 (m), 2885 (m), 2831 (w), 1597 (w), 1481 (w), 1388 (w), 1350 (w), 1134 (m), 1087 (s), 1033 (s), 894 (m), 848 (s), 763 (m), 702 (s). The structure of **9** was also confirmed by the X-ray structure determination. Anal. calcd for $C_{42}H_{70}FeO_4 \cdot H_2O$: C, 70.76; H, 10.18. Found: C, 69.92; H, 9.78.

Synthesis of Ru(cymene)[(κ^2-OC^{t}Bu$_2$Me$_2$C$_6$H$_2$)] (10)

A solution of Tl$_2$(OC^{t}Bu$_2$(3,5-Me$_2$C$_6$H$_3$))$_2$ (133 mg, 0.147 mmol) in THF was added to a stirred THF solution of [Ru(*p*-cymene)Cl$_2$]$_2$ (45 mg, 0.074 mmol) at room temperature. Following the addition, the solution turned magenta and precipitate formation was observed. The reaction was stirred at room temperature for one hour. The volatiles were removed *in vacuo*. The resulting residue was dissolved in hexane, filtered, and concentrated. Recrystallization from hexane at −35 °C yielded dark purple X-ray quality crystals of **10** (59 mg, 81% yield). ^{1}H NMR (C_6D_6, 600 MHz) δ 7.27 (s, 1H, Ph), 7.01 (s, 1H, Ph), 5.55 (d, J_{HH} = 6.2 Hz, 2H, cymene), 5.42 (d, J_{HH} = 6.2 Hz, 2H, cymene), 3.09 (s, 3H, Me), 2.21 (s, 3H, Me), 1.57 (s, 3H, Me), 1.95 (sept, J_{HH} = 6.7 Hz, 1H, ^{i}Pr), 1.43 (s, 3H, Me) 1.20 (s, 18H, ^{t}Bu), 0.97 (d, J_{HH} = 6.7 Hz, 6H, ^{i}Pr) ppm. ^{13}C NMR (C_6D_6, 150 MHz) δ 176.88, 171.10, 149.55, 131.34, 127.73, 123.06, 106.48, 90.20, 84.55, 82.99, 78.88, 39.96, 32.54, 31.45, 30.56, 23.37, 22.35, 20.44 ppm. UV-vis: λ_{max}, nm (ε_M, L mol^{-1} cm^{-1}): 545 (5200), 361 (15 400), 263 (30 000). The structure of **10** was also confirmed by the X-ray structure determination.

Conflicts of interest

There are conflicts of interest to declare.

Acknowledgements

References

1 D. C. Bradley, R. C. Mehrotra, I. Rothwell and A. Singh, *Alkoxo and Aryloxo Derivatives of Metals*; Academic Press, London, UK, 2001.

2 N. Y. Turova, E. P. Turevskaya, V. G. Kessler and M. I. Yanovskaya, The Chemistry of Metal Alkoxides, Springer, New York, NY, 2002.

3 R. C. Mehrotra, A. Singh and S. Sogani, *Chem. Soc. Rev.*, 1994, **23**, 215–225.

4 R. R. Schrock and C. Copéret, *Organometallics*, 2017, **36**, 1884–1892.

5 R. R. Schrock, High Oxidation State Molybdenum and Tungsten Complexes Relevant to Olefin Metathesis, in *Handbook of Metathesis*, ed. R. H. Grubbs and A. G. Wenzel, Wiley-VCH, Weinheim, 2nd edn, 2015, vol 1, pp. 1–32.

6 S. E. N. Brazeau and L. H. Doerrer, *Dalton Trans.*, 2019, **48**, 4759–4768.

7 P. T. Wolczanski, *Polyhedron*, 1995, **14**, 3335–3362.

8 J. A. Bellow, M. Yousif and S. Groysman, *Comments Inorg. Chem.*, 2015, **36**, 92–122.

9 K. G. Caulton and L. G. Hubert-Pfalzgraf, *Chem. Rev.*, 1990, **90**, 969–995.

10 M. V. Petersen, A. H. Iqbal, L. N. Zakharov, A. L. Rheingold and L. H. Doerrer, *Polyhedron*, 2013, **52**, 276–283.

11 J. S. Lum, P. E. Chen, A. L. Rheingold and L. H. Doerrer, *Polyhedron*, 2013, **58**, 218–228.

12 A. Grass, D. Wannipurage, R. L. Lord and S. Groysman, *Coord. Chem. Rev.*, 2019, **400**, 1–16.

13 J. A. Bellow, D. Fang, N. Kovacevic, P. D. Martin, J. Shearer, G. A. Cisneros and S. Groysman, *Chem. – Eur. J.*, 2013, **19**, 12225–12228.

14 J. A. Bellow, M. Yousif, D. Fang, E. G. Kratz, G. A. Cisneros and S. Groysman, *Inorg. Chem.*, 2015, **54**, 5624–5633.

15 D. C. Bradley, M. B. Hursthouse, C. W. Newing and A. J. Welch, *J. Chem. Soc., Chem. Commun.*, 1972, 567–568.

16 M. Yousif, D. J. Tjapkes, R. L. Lord and S. Groysman, *Organometallics*, 2015, **34**, 5119–5128.

17 T. S. Hollingsworth, R. L. Hollingsworth, T. Rosen and S. Groysman, *RSC Adv.*, 2017, **7**, 41819–41829.

18 D. Wannipurage, T. S. Hollingsworth, F. Santulli, M. Cozzolino, M. Lamberti, S. Groysman and M. Mazzeo, *Dalton Trans.*, 2020, **49**, 2715–2723.

19 V. Kumar, V. Singh, A. N. Gupta, M. G. B. Drew and N. Singh, *Dalton Trans.*, 2015, **44**, 1716–1723.

20 H. Rothfuss, K. Folting and K. G. Caulton, *Inorg. Chim. Acta*, 1993, **212**, 165–173.

21 C. A. Zechmann, T. J. Boyle, D. M. Pedrotty, T. M. Alam, D. P. Lang and B. L. Scott, *Inorg. Chem.*, 2001, **40**, 2177–2184.

22 T. J. Boyle, C. A. Zechmann, T. M. Alam, M. A. Rodriguez, C. A. Hijar and B. L. Scott, *Inorg. Chem.*, 2002, **41**, 946–957.

23 F. Blasberg, H.-W. Lerner and M. Bolte, *Acta Crystallogr., Sect. E: Struct. Rep. Online*, 2010, **66**, m1621, DOI: 10.1107/S1600536810047550.

24 J. S. Lum, L. Tahsini, J. A. Golen, C. Moore, A. L. Rheingold and L. H. Doerrer, *Chem. – Eur. J.*, 2013, **19**, 6374–6384.

25 H. W. Roesky, M. Scholz, M. Noltemeyer and F. T. Edelmann, *Inorg. Chem.*, 1989, **28**, 3829–3830.

26 Z. Zhu, R. J. Wright, Z. D. Brown, A. R. Fox, A. D. Phillips, A. F. Richards, M. M. Olmstead and P. P. Power, *Organometallics*, 2009, **28**, 2512–2519.

27 K. Akhbari and A. Morsali, *CrystEngComm*, 2012, **14**, 1618–1628.

28 A. A. El-Hadad, J. E. Kickham, S. J. Loeb, L. Taricani and D. G. Tuck, *Inorg. Chem.*, 1995, **34**, 120–123.

29 K. Akhbari and A. Morsali, *Polyhedron*, 2011, **30**, 2459–2465.

30 M. V. Childress, D. Millar, T. M. Alam, K. A. Kreisel, G. P. A. Yap, L. N. Zakharov, J. A. Golen, A. L. Rheingold and L. H. Doerrer, *Inorg. Chem.*, 2006, **45**, 3864–3872.

31 J. M. Harrowfield, R. P. Sharma, B. W. Skelton and A. H. White, *Aust. J. Chem.*, 1998, **51**, 735–746.

32 A. Askarinejad and A. Morsali, *Inorg. Chem. Commun.*, 2006, **9**, 143–146.

33 J. A. Bellow, P. D. Martin, R. L. Lord and S. Groysman, *Inorg. Chem.*, 2013, **52**, 12335–12337.

34 P. P. Power and S. C. Shoner, *Angew. Chem., Int Ed. Engl.*, 1990, **29**, 1403–1404.

35 M. Bochmann, G. C. Bwembya, R. Grinter, A. K. Powell, K. J. Webb, M. B. Hursthouse, K. M. A. Malik and M. A. Mazid, *Inorg. Chem.*, 1994, **33**, 2290–2296.

36 M. Westerhausen, B. Rademache and W. Schwarz, *Z. Anorg. Allg. Chem.*, 1993, **619**, 675–689.

37 E. Martin, D. L. Hughes and S. J. Lancaster, *Eur. J. Inorg. Chem.*, 2006, 4037–4041.

38 J. J. Ellison, K. Ruhlandt-Senge, H. H. Hope and P. P. Power, *Inorg. Chem.*, 1995, **34**, 49–54.

39 G. Zhu, J. M. Tanski and G. Parkin, *J. Chem. Crystallogr.*, 2002, **32**, 469–475.

40 A. Hernán-Gómez, E. Herd, M. Uzelac, T. Cadenbach, A. R. Kennedy, I. Borilovic, G. Aromí and E. Hevia, *Organometallics*, 2015, **34**, 2614–2623.

41 G. Anantharaman and K. Elango, *Organometallics*, 2007, **26**, 1089–1092.

42 D. J. Darensbourg, S. A. Niezgoda, J. D. Draper and J. H. Reibenspies, *Inorg. Chem.*, 1999, **38**, 1356–1359.

43 D. J. Darensbourg, M. S. Zimmer, P. Rainey and D. L. Larkins, *Inorg. Chem.*, 1998, **37**, 2852–2853.

44 P. Jochmann and D. W. Stephan, *Chem. – Eur. J.*, 2014, **20**, 8370–8378.

45 S. A. Cantalupo, J. S. Lum, M. C. Buzzeo, C. Moore, A. G. Di Pasquale, A. L. Rheingold and L. H. Doerrer, *Dalton Trans.*, 2010, **39**, 374–383.

46 J. R. Fulton, A. W. Holland, D. J. Fox and R. G. Bergman, *Acc. Chem. Res.*, 2002, **35**, 44–56.

47 M. S. Sanford, L. M. Henling, M. W. Day and R. H. Grubbs, *Angew. Chem., Int. Ed.*, 2000, **39**, 3451–3453.

48 C. Melero, L. M. Martınez-Prieto, P. Palma, D. del Rio, E. A. lvareza and J. Campora, *Chem. Commun.*, 2010, **46**, 8851–8853.

49 C. C. Comanescu and V. M. Iluc, *Organometallics*, 2014, **33**, 6059–6064.

50 I. Matas, J. Cámpora, P. Palma and E. Álvarez, *Organometallics*, 2009, **28**, 6515–6523.

51 M. Yousif, D. Wannipurage, C. D. Huizenga, E. Washnock-Schmid, N. J. Peraino, A. Ozarowski, S. A. Stoian, R. L. Lord and S. Groysman, *Inorg. Chem.*, 2018, **57**, 9425–9438.

52 G. M. Sheldrick, *Acta Crystallogr., Sect. C: Struct. Chem.*, 2015, **71**, 3–8.

53 O. V. Dolomanov, L. J. Bourhis, R. J. Gildea, J. A. K. Howard and H. Puschmann, *J. Appl. Crystallogr.*, 2009, **42**, 339–341.